

Femtosecond electron dynamics at the benzene/Ag(111) interface

K.J. Gaffney, C.M. Wong, S.H. Liu, A.D. Miller, J.D. McNeill, C.B. Harris *

Department of Chemistry, University of California, Berkeley, CA 94720, USA

Chemical Sciences Division, E.O. Lawrence Berkeley National Laboratory, Berkeley, CA 94720, USA

Received 3 March 1999

Abstract

The layer dependent evolution of the benzene/Ag(111) unoccupied electronic structure and electron dynamics have been investigated with time and angle resolved two photon photoemission. With the exception of one peak in the benzene multilayer photoelectron kinetic energy spectra, all excitations possess free electron-like dispersions parallel to the Ag(111) surface, consistent with image electronic states and not electron affinity levels in benzene molecular crystals. The non-dispersive peak in the benzene multilayer spectra is assigned to be an $n = 1$ image state localized by structural disorder. The binding energy and lifetime of the $n = 1$ image state has been measured for 1 to 5 layers of benzene. Adsorption of a benzene monolayer moves the $n = 1$ image state electron closer to the metal, raising the $n = 1$ binding energy from -0.77 eV to -0.84 eV and lowering the $n = 1$ lifetime from 36 to 20 femtoseconds. Adsorption of a bilayer lowers the $n = 1$ binding energy to -0.68 eV and raises the $n = 1$ lifetime to 45 fs. The lifetime and binding energy remain constant from a bilayer to 5 layers of benzene. A dielectric continuum model successfully reproduces these trends in $n = 1$ binding energy and lifetime. Analysis of the model potential and the calculated wavefunctions shows the layer independence of the multilayer $n = 1$ lifetimes and binding energies to result from the trapping of the image state electron in the screened image potential within the benzene layer. © 2000 Elsevier Science B.V. All rights reserved.

1. Introduction

The electronic structure and lifetime of excess electrons in molecular adsorbate layers on metal surfaces influence the function of many fundamental and technologically significant processes, including photochemistry at metal surfaces and charge injection in light emitting diodes (LEDs). Molecular anion formation via electron transfer from the metal substrate has been implicated as the initial step in photodissociation and photodesorption at metal surfaces [1,2] while the charge injection event in or-

ganic LEDs composed of aromatic and conjugated molecules [3] depends on the interfacial band structure and the electron transfer dynamics [4]. Time and angle resolved two photon photoemission (TPPE) provides an opportunity to investigate the dynamics of interfacial electron transfer with electronic state specificity. Our study of the benzene/Ag(111) system emphasizes the layer dependent evolution of the interfacial electronic structure, the influence of the benzene electron affinity on the electron transfer rate, and illustrates the importance of time and angle resolution in the study of interfacial phenomena.

Adsorbate electron affinity levels modify the image potential and influence the interfacial electronic structure and electron transfer dynamics. The well

* Corresponding author.

characterized adsorbate crystal structure and weak benzene/Ag(111) electronic interaction assists the determination of the benzene coverage and supports the use of bulk benzene parameters for modeling the influence of the benzene layer on the interfacial image potential. Despite the extensive study of the excited electronic structure of benzene adsorbed on noble metal surfaces [5–8], the influence of the benzene first electron affinity level on the image potential has yet to be modeled successfully. Image states form delocalized two dimensional bands, while electron affinity levels in aromatic molecular crystals form narrow electronic bands. The validity of assigning the excitations in the angle resolved TPPE photoelectron kinetic energy spectra as image states is clearly supported by the binding energies and dispersions reported in Section 5. Benzene molecular anions did not appear in our TPPE study of the benzene/Ag(111) interface [9]. With the exception of one peak in the benzene multilayer spectra, all excitations possess free electron-like dispersions parallel to the Ag(111) surface, consistent with image electronic states and not with excess electrons in aromatic molecular crystals [9]. A localized, non-dispersive peak in the benzene multilayer spectra results from structural disorder induced image state localization, as discussed in Section 5.

The study of the benzene/Cu(111) interface conducted by Velic et al. constitutes the first angle and time resolved TPPE investigation of the unoccupied electronic structure of benzene adsorbed on a noble metal surface [8]. They observed a final state resonance in the TPPE kinetic energy spectra which they assign to be the benzene first electron affinity level, and measured the binding energy, effective mass, and lifetime of the $n = 1$ image state for a monolayer and bilayer of benzene. Velic et al. do not report results for higher image states or coverages exceeding a bilayer. The $n = 1$ binding energies and lifetimes were modeled with a dielectric continuum model [10]. The assignment of the final state resonance as the benzene electron affinity level dictates the use of the repulsive benzene gas phase electron affinity in the model calculation, but results in $n = 1$ image state lifetimes orders of magnitude too long. Section 7 discusses the importance of using condensed phase electron affinities in the dielectric continuum model.

The current study represents the first investigation of the layer dependent evolution of the unoccupied electronic structure of the benzene/Ag(111) interface. Studies of the Xe/Ag(111) and the *n*-heptane/Ag(111) interfaces have shown that layer dependent changes in image state properties, particularly lifetimes, provide the key information for modeling interfacial dielectric/metal electronic structure [11]. The $n = 1$ binding energy increases and lifetime decreases upon the adsorption of the benzene monolayer, indicating that adsorption of the benzene monolayer moves the $n = 1$ image state electron closer to the Ag(111) surface. Adsorption of a bilayer decreases the binding energy and increases the lifetime. The $n = 1$ lifetime and binding energy do not change when the benzene coverage increases from a bilayer to 5 layers. Sections V and VI discuss these results in greater detail. Section 7 contains a dielectric continuum model calculation of the $n = 1$ binding energy and lifetime as a function of layer thickness. The model successfully reproduces the layer dependent trends in $n = 1$ lifetime and binding energy, but incorrectly predicts a transition from image states to benzene quantum wells for the higher image states. Image states with energies higher than that of the layer electron affinity (see Fig. 1) form

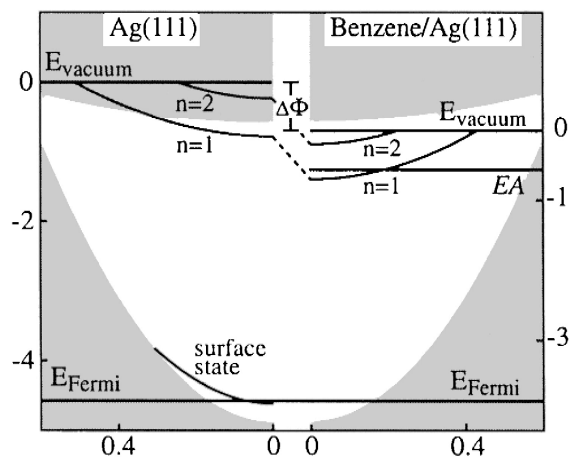


Fig. 1. Projected bulk band structure for Ag(111) is shown to the left and multilayer benzene/Ag(111) to the right. The change in workfunction, $\Delta\Phi$, moves the vacuum energy, E_{vac} , towards the center of the substrate band gap. The benzene first electron affinity level, EA , is pictured to the right. The EA binding energy of -0.6 eV is less than that of $n = 1$, but more than that of $n = 2$.

quantum wells at the Xe/Ag(111) interface which possesses a dispersive conduction band [10], but not at the benzene/Ag(111) interface. The lack of benzene quantum well formation may reflect the narrow electronic bands of aromatic molecular crystals, but the lack of sophisticated electronic band structure calculations makes such a determination difficult [9].

2. TPPE experimental technique

Time and angle resolved TPPE involves the excitation of electrons from occupied metal orbitals to unoccupied interfacial states with an excitation pulse and photoemission of the excited electrons with a probe pulse. Measuring the number of electrons detected as a function of time delay between the arrival of the excitation and probe pulses determines the lifetime of transient electronic states. Measuring the photoemitted electron's kinetic energy, E_{kin} , as a function of angle, θ , determines the electronic state's effective mass, m^* . Free electron-like states possess parabolic dispersion, $E_{\text{kin}} = E_0 + \hbar^2 k_{\parallel}^2 / 2m^*$, where $k_{\parallel} = \sqrt{2m_e E_{\text{kin}} / \hbar^2} \sin \theta$ is the wave vector parallel to the interface and E_0 is the kinetic energy for photoemission normal to the interface. Localized electronic states have angle independent kinetic energies.

Before discussing the results of our experiment in detail, a brief description of the time and momentum resolved TPPE experimental design is in order. Time of flight single electron counting detection with a low power, high repetition rate laser minimizes space charge broadening. An energy resolution of roughly 20 meV results from the uncertainty in the electron time of flight. The published errors in the binding energies reflect the experimental variation in the measured values. Visible light femtosecond (fs) pulses, tunable from 470 to 730 nm, are generated in an optical parametric amplifier (OPA). The OPA outputs 70 fs pulses with 100 nJ per pulse at a 200 kHz repetition rate for 650 nm light. The visible light is frequency doubled in a BBO crystal to generate ultraviolet (UV) light pulses. The remaining visible light is diverted from the UV light with a dichroic mirror. The arrival of the visible light pulse at the sample can be delayed with respect to the UV light

pulse by changing the path length of the visible light with a translation stage. The UV and visible light pulses are spatially overlapped with a second dichroic mirror and focused on the sample in a vacuum chamber. The instrument response function must be determined to calculate excited state electronic lifetimes from the time resolved data. The dynamics of the Ag(111) occupied surface state when excited to a virtual intermediate state and the non-resonant background signal are utilized for this purpose. The instrument response function exhibits a gaussian profile with an average full width at half maximum of 100 fs. Image state lifetimes are determined by convolving the instrument response function with a single exponential decay. The laser pulses are *p*-polarized and impinge on the sample 60° from the surface normal. The vacuum chamber has a base pressure of 6×10^{-11} Torr. Multiple freeze, pump, and thaw cycles insure the high purity of the benzene vapor introduced into the ultrahigh vacuum chamber via a leak valve. All reported exposures in Langmuir reflect the uncorrected pressure gauge readings. Sample preparation involves sputtering and annealing cycles, with the cleanliness of the surface monitored by TPPE and Auger electron spectroscopy (AES). Surface characterization is achieved with low energy electron diffraction (LEED), AES, mass spectrometry, and TPPE. More detailed descriptions of our experimental apparatus can be found in a previous account [11].

3. Benzene layer growth and workfunction change determination

The adsorption of benzene on Ag(111) has been investigated with a multitude of techniques and many aspects of benzene layer growth have been determined. These previous studies, in conjunction with in situ LEED and TPPE analysis, are used to determine the benzene coverage. Benzene physisorbs molecularly on Ag(111) with the plane of the molecule parallel to the interface [12,13]. Ordered LEED patterns for benzene appear below 160 K in the presence of a 5×10^{-8} Torr benzene back pressure, consistent with the work of Somorjai and Firment [14]. The growth of a monolayer and a bilayer

is determined by monitoring the dose dependent LEED pattern at 120 K. For a dosage of 1 to 4 Langmuir at 120 K no overlayer LEED pattern is observable, while a dosage of 5 to 6 Langmuir results in a LEED pattern consistent with the (3×3) benzene monolayer LEED pattern reported by Dudde et al. for a dosage of 5 Langmuir [13]. An additional 12 Langmuir results in a new hexagonal LEED pattern commensurate with the substrate and possessing a larger unit cell than the monolayer pattern. The pattern cannot be due to a more densely packed monolayer because the unit cell increases, rather than decreases, in size. This pattern results from the formation of a stable bilayer at 120 K. Neither the LEED pattern nor the TPPE spectra change when the benzene dosage exceeds 18 Langmuir, leading to the conclusion that only a bilayer will persist at 120 K, Fig. 2. This is the first observation of a stable bilayer of benzene adsorbed on Ag(111), though a stable bilayer has been observed on Cu(111) by Bent and coworkers [15]. Benzene coverage in excess of a bilayer was grown at 80 K. The change in workfunction and $n = 1$ effective mass are utilized to determine the transition from a bilayer to a trilayer of benzene. To increase the benzene coverage from a

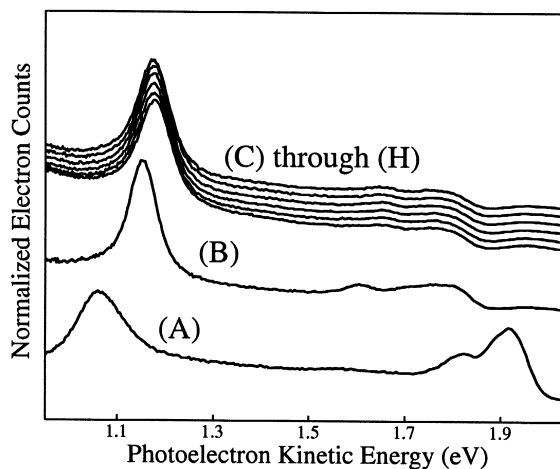


Fig. 2. Dose dependent photoelectron kinetic energy spectra at 120 K. The pictured spectra result from the following cumulative doses: (A) 6 Langmuir, (B) 12 Langmuir, and (C) through (H) 18 to 120 Langmuir. Spectra (A) corresponds to a monolayer, while (C) through (H) correspond to a bilayer of benzene adsorbed on Ag(111).

bilayer to a trilayer requires an additional 15 Langmuir. Coverage in excess of a trilayer is estimated from the dose dependence of the trilayer. All reported multilayer data were collected after the layer annealed to the point where the localized excitation was no longer observed.

Workfunction determination must be achieved to determine the binding energy of the transient electronic states in the TPPE kinetic energy spectra. This was achieved with two approaches. The first approach involves fitting the image state energy separations to a quantum defect parameter a , $E = -0.85/(n + a)^2$ eV, which in turn gives the image state binding energies. The extent by which the image state binding energies differ from the predicted values gives the change in workfunction. The second method involves determining the TPPE kinetic energy width for an accelerating voltage bias between the sample and the detector so that both a high and a low energy cut-off are present in the kinetic energy spectra. Only UV light at a frequency that disallows single photon photoemission is used and the TPPE kinetic energy width is subtracted from the energy of two UV photons to determine the workfunction. The second method gave a workfunction change of -0.7 ± 0.1 eV for a monolayer of benzene and no measurable change for multilayer adsorption. The quantum defect method gave workfunction changes of -0.65 ± 0.02 eV for a monolayer of benzene, -0.07 ± 0.02 eV for a bilayer, and $+0.04 \pm 0.02$ eV for a trilayer of benzene. Cited binding energies were determined with the quantum defect analysis. Our change in workfunction measurements lie between the values of Zhou et al. [16], -0.7 eV for a monolayer of benzene and -0.2 eV for multilayer benzene, and Dudde et al. [13], -0.3 eV for a monolayer of benzene.

4. Prior studies of the excited electronic structure of benzene adsorbed on noble metal surfaces

Previous investigations of the excited electronic structure of benzene physisorbed on noble metal surfaces provide key information that complements and enhances the interpretation of our time and angle resolved TPPE results. Frank et al. conducted IPS

studies of the excited electronic states of 2–3 layers of benzene adsorbed on Ag(111) [5]. They found the energies of the first and second electron affinity levels to be 0.6 eV and -3.2 eV. The dielectric continuum model of Section 7 confirms that benzene adsorbed on Ag(111) has an attractive first electron affinity of 0.6 eV. The energy spacing between the electron affinity levels of benzene, as well as other aromatic molecules, adsorbed on Ag(111) were found to be similar to the energy spacing between the same electron affinity levels in the gas phase, supporting the conclusion that the silver substrate only weakly perturbs the electronic structure of aromatic adsorbates. The 1.7 eV shift to larger electron affinities for adsorbed, as opposed to gas phase, benzene is attributed to anion stabilization by the polarizable benzene adlayer and the silver substrate image potential. The peak in the IPS study assigned to be the first electron affinity level may be the peak assigned as the multilayer $n = 1$ image state in the current study, but the lack of angle resolved data in the IPS study makes distinguishing between molecular anions and image states difficult.

Two recent studies utilized TPPE to investigate the benzene/Cu(111) interface. Munakata et al. studied 0.3 Langmuir of benzene dosed at 100 K with static TPPE [6,7]. The TPPE study identified the ionization potential of the first triplet excited state of benzene adsorbed on Cu(111) and possibly a vibrational progression, but did not report any benzene anion states or image potential states. We did not observe any intramolecular benzene electronic transitions.

The Velic et al. study focused on a coverage of 1.5 layers of benzene on Cu(111) with time and angle resolved TPPE [8]. This coverage simultaneously supports $n = 1$ image states for both monolayer and bilayer benzene, as well as the benzene first electron affinity level 0.6 eV above the vacuum level. This marks the first observation of a final state resonance with TPPE. Why the first electron affinity level of benzene lies 1.2 eV higher in energy for physisorption on Cu(111) than it does for physisorption on Ag(111) [5] remains unclear. The $n = 1$ lifetime for the monolayer and bilayer $n = 1$ state were measured to be 40 fs and 20 fs, respectively. The image state binding energies and lifetimes were modeled with a dielectric continuum model. The

model calculation suggests that the $n = 1$ bilayer lifetime should be three orders of magnitude longer than the $n = 1$ monolayer lifetime, rather than halved.

Other studies confirm that the benzene adsorbate interacts weakly with the Ag(111) surface, leaving the majority of benzene electronic properties only weakly perturbed. Molecular orbital calculations by Anderson et al. indicate that benzene and the Ag(111) surface have a non-bonding interaction [17]. The electron energy loss spectroscopy (EELS) studies of 0.4 Langmuir benzene on the Ag(111) surface conducted by Avouris and Demuth found that benzene electronic transition energies are only weakly perturbed from their gas phase values by the Ag(111) substrate [12], while the UV photoemission spectra of benzene adsorbed on Ag(111) strongly resembles that of gas phase benzene [13]. The lack of electronic perturbation of the adsorbate by the substrate allows comparisons between bulk benzene electronic properties and the electronic properties of the adsorbed layers and validates the use of bulk benzene parameters in the dielectric continuum model calculations of Section 7.

5. Excited electronic states at the benzene/Ag(111) interface

The adsorbate and substrate electronic structure, depicted in Fig. 1, influence the binding energy, effective mass, and lifetime of image state electrons at the benzene/Ag(111) interface. The electron affinity, and to a lesser extent the dielectric constant, play a critical role in determining the effect of the benzene layer on the interfacial image states [11]. Fig. 3 shows the kinetic energy spectra for a monolayer, a bilayer, and a trilayer of benzene physisorbed on Ag(111). Image state electrons dominate the spectra, along with the occupied surface state for the benzene monolayer. Layer adsorption generally moves the Ag(111) occupied surface state above the Fermi level due to quantum confinement, though the Ag(111) surface state does persist in the presence of a Kr monolayer. The binding energy and effective mass of image states at dielectric/metal interfaces reflect the influence of the adsorbate layer on the interfacial image potential. Table 1 lists these quantities for various layer thicknesses of benzene

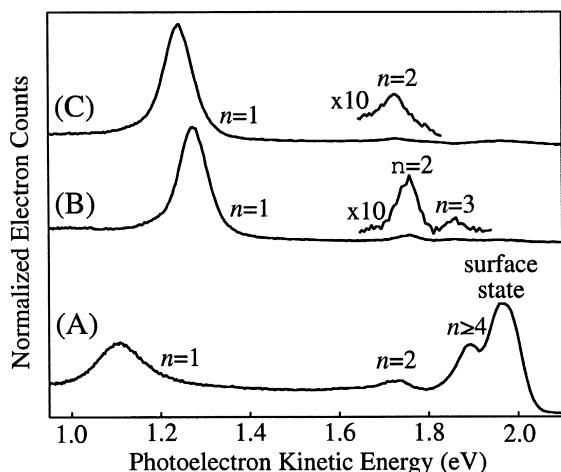


Fig. 3. Photoelectron kinetic energy spectra for a monolayer (A), a bilayer (B), and a trilayer (C) of benzene adsorbed on Ag(111). Variations in the photoelectron kinetic energy reflect variations in wavelength, workfunction, and binding energy. The persistence of the occupied surface state for the monolayer coverage results in the resonant excitation of $n \geq 4$ with 3.9 eV photons. Image state binding energies are reported in Table 1.

on the Ag(111) surface. The adsorption of a monolayer of benzene results in an increase in the binding energy of the $n = 1$ image state, but a decrease in the $n = 2$ binding energy. On the clean surface, the $n = 2$ binding energy of -0.23 eV exceeds the hydrogenic value due to degeneracy with the projected bulk conduction band [18], Fig. 1. Adsorption of a monolayer of benzene decreases the $n = 2$ binding energy because the decrease in workfunction breaks the degeneracy between $n = 2$ and the substrate conduction band. The $n = 1$ binding energy of -0.68 eV for benzene coverage in excess of a monolayer is less than the $n = 1$ binding energy of -0.77 eV for the Ag(111) surface. The $n = 1$ bind-

Table 1
Experimental and calculated results for $n = 1$

	Binding energy (eV)		Lifetime (fs)	
	Experimental	Calculated	Experimental	Calculated
1 ML	-0.84	-0.89	20	16
2 ML	-0.68	-0.71	45	61
3 ML	-0.68	-0.68	50	45
4 ML	-0.68	-0.71	50	45
5 ML	-0.68	-0.72	50	51

ing energy remains constant from a bilayer to 5 layers of benzene. The $n = 1$ binding energy of -0.80 eV for a monolayer and -0.65 eV for a bilayer of benzene on Cu(111) differ little from those of the current study [8]. Velic et al. did not report results for benzene coverage greater than a bilayer.

The layer dependent evolution of the effective mass of the $n = 1$ image state has been investigated with angle resolved TPPE. The effective mass of the image states parallel to the interface remain free electron-like for the majority of the dielectric/Ag(111) interfaces studied by Harris and coworkers [11]. The effective mass of $n = 1$ decreases upon adsorption of benzene, Fig. 4. A major cause for the change in the effective mass is the change in workfunction. The decrease in workfunction lessens the image state interaction with the substrate conduction band (see Fig. 1), which results in the decreased effective mass [19]. This effect cannot, however, account for a monolayer effective mass of less than 1 or the increase in the effective mass for the transitions from monolayer to bilayer benzene and bilayer to trilayer benzene, Fig. 4. The $n = 1$ effective mass does not change above a trilayer of benzene. These subtle variations in effective mass most likely result from the $n = 1$ image state interaction with the adsorbate layer parallel to the interface. The monolayer

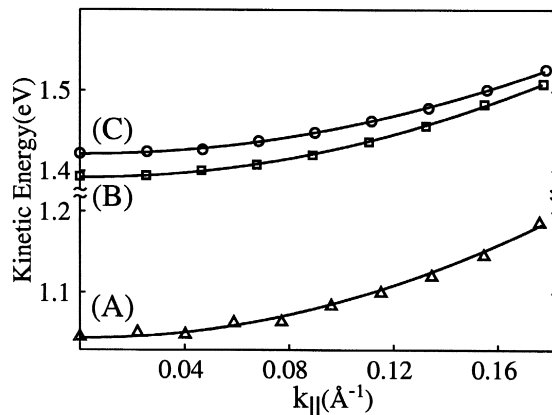


Fig. 4. The dispersion of the $n = 1$ image state for a monolayer (A), bilayer (B), and trilayer (C) of benzene adsorbed on Ag(111). The measured effective masses are 0.9 ± 0.1 , 1.0 ± 0.1 , and 1.2 ± 0.2 for a monolayer, bilayer, and trilayer, respectively. The $n = 1$ image state has an effective mass of 1.3 for the clean Ag(111) surface.

$n = 1$ effective mass of 0.9 resembles the 1.1 value measured by Velic et al., but the bilayer value of 1.0 differs significantly from the $n = 1$ effective mass of 1.9 found for a bilayer of benzene adsorbed on Cu(111) [8].

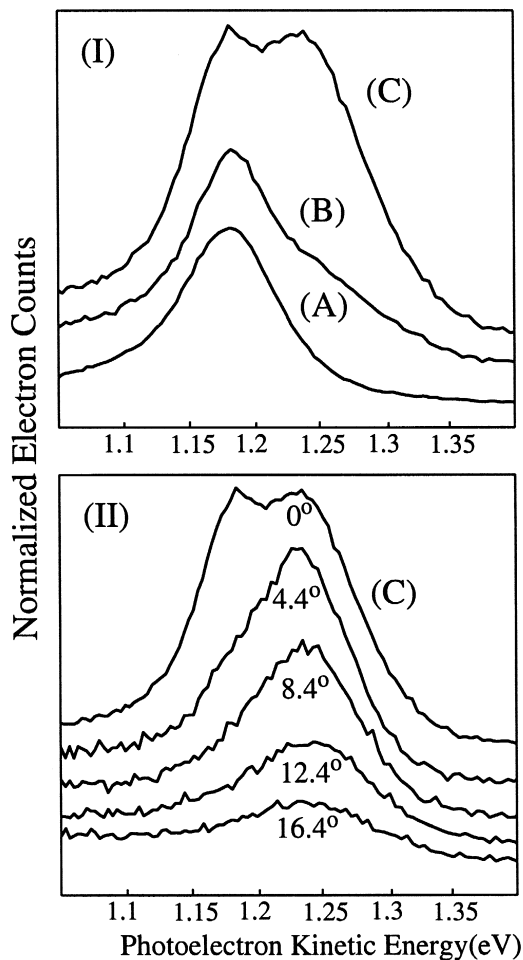


Fig. 5. The development of the localized $n = 1$ image state as a function of coverage appears in (I) with (A) corresponding to a bilayer, (B) 3.5 layers, and (C) 4 layers of benzene. The two peaks in (C), from right to left, correspond to the localized state and the delocalized $n = 1$ image state. The photoelectron kinetic energy spectra of 4 layers of benzene adsorbed on Ag(111) as a function of angle appear in (II). The delay time between the excitation and probe pulses is 70 fs for the 0° spectra and 170 fs for all other angles. The longer delay time allows the localized state, which possesses a slightly longer lifetime, to dominate the kinetic energy spectra. The invariance of the photoelectron kinetic energy of the primary peak in (II) confirms the state to be localized parallel to the interface.

For benzene coverage in excess of a bilayer, a new excited electronic state appears in the kinetic energy spectra, Fig. 5. The new excitation possesses an angle independent photoelectron kinetic energy, indicating that the state is spatially localized parallel to the interface, Fig. 5. Three criteria support the conclusion that the peak results from structural disorder induced localization of the $n = 1$ image state. Foremost, the excitation slowly shrinks in magnitude as the layer anneals. This annealing occurs at a temperature too low for benzene desorption, so the localized peak would appear to diminish as the layer disorder diminishes. Secondly, the peak requires p -polarized light to be photoemitted consistent with the symmetry requirements for photoemission of image states. Lastly, the lower binding energy of the localized $n = 1$ image state, when compared to the dispersive $n = 1$ image state, is consistent with the effect of disorder induced quantum confinement parallel to the interface. A similar increase in image state energy was found for image states localized on Ag(111) islands adsorbed on a Pd(111) surface [20]. Interestingly, for disorder induced localization of image states at the benzene/Ag(111) interface the localization either has no time dependence or localizes too fast to detect, whereas image state localization via small polaron formation at the n -heptane/Ag(111) interface occurs dynamically [21].

6. Excited electronic state dynamics for the benzene/Ag(111) interface

In addition to monitoring the layer dependent electronic structure, time resolved TPPE allows for the measurement of excited state lifetimes. The determination of the time scale for electron relaxation indicates the extent of coupling between the excited interfacial electron and the Ag(111) substrate. A physisorbed insulator, such as benzene on Ag(111), should lack low lying unoccupied electronic levels into which image state electrons can decay. To first approximation, the image state electron relaxation at the benzene/Ag(111) interface will be dominated by electron hole excitation in the metal, resulting in lifetimes proportional to the the image state wavefunction overlap in the metal. Partially occupied

surface states provide a decay path for image state electrons at the benzene/Ag(111) interface, but accounting for this effect involves a more sophisticated theoretical description of surface electron relaxation than the one presented in Section 7 [22,23]. Table 1 details the layer dependent evolution of the image state lifetimes for the benzene/Ag(111) interface. The $n = 1$ lifetime for a monolayer of benzene on Ag(111) is shorter than the $n = 1$ lifetime of 36 fs for the clean Ag(111) surface. This result suggests that adsorption of a benzene monolayer moves the $n = 1$ image state closer to the Ag(111) surface. The adsorption of a benzene monolayer also increases the $n = 1$ binding energy, which also supports the conclusion that the adsorption of the monolayer moves the $n = 1$ electron closer to the Ag(111) surface. The $n = 1$ lifetime increases to 45 fs for a bilayer of benzene. This result should be contrasted with that of Velic et al., where the bilayer $n = 1$ lifetime is half that of the monolayer lifetime. The 20 fs and 45 fs $n = 1$ lifetimes for mono- and bilayer benzene on Ag(111) measured in the current study are roughly the reverse of those for mono- and bilayer benzene on Cu(111) reported by Velic et al., 40 fs and 17 fs respectively [8]. Fig. 6 illustrates the lack of change

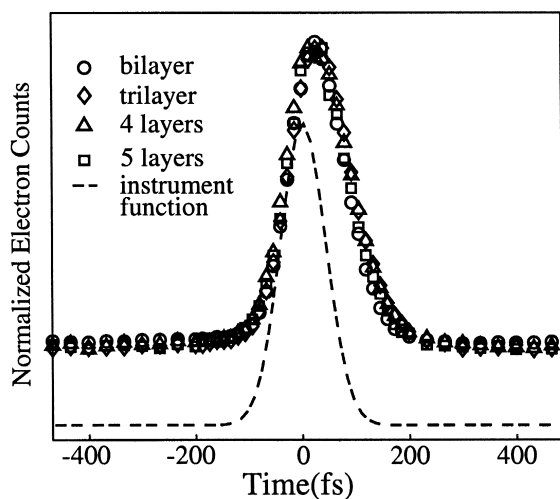


Fig. 6. The instrument function and fs population dynamics of the $n = 1$ image state for 2 to 5 layers of benzene adsorbed on Ag(111). The dynamic traces clearly show the similarity of the $n = 1$ population dynamics for 2 to 5 layers of benzene. The $n = 1$ dynamics are fit by convolving the instrument function with an exponential decay. The $n = 1$ lifetimes are reported in Table 1.

in the $n = 1$ lifetime when the benzene coverage increases from a bilayer to 5 layers. Lifetimes comparable to the clean Ag(111) surface and the lack of decay channels within the benzene layer necessitate a large electron density near the benzene/Ag(111) interface.

7. Model calculation of binding energies and lifetimes for the benzene/Ag(111) interface

The dielectric continuum model employed by McNeill et al. to model the unoccupied electronic structure of the Xe/Ag(111) [10] interface successfully reproduces the layer dependent trends in $n = 1$ binding energies and lifetimes for the benzene/Ag(111) interface. The model represents the electronic structure of the dielectric layer with an electron affinity and a dielectric constant, and accounts for the effect of the dielectric layer on image state binding energies and lifetimes without considering the band structure of the adsorbate. The model as employed by Harris and coworkers for Xe, n-heptane, and presently benzene uses the free electron mass to determine the electron kinetic energy in the layer [11] rather than treating the electron mass as an adjustable parameter [24]. McNeill et al. present the equations for constructing the model potential used for the present calculation. Fig. 7 presents the interfacial potential used for the benzene/Ag(111) interface.

The dielectric continuum model potential must be modified to avoid singularities at the metal/dielectric and the dielectric/vacuum interfaces. To avoid the singularity at the metal/dielectric interface, the potential is cut-off at the Fermi energy near the metal surface. The singularity at the dielectric/vacuum interface is eliminated by linearly interpolating the potential between $V(t - b/2)$ and $V(t + b/2)$, where t represents the layer thickness and b is the width of the interpolation. The calculations reported herein set b to 3 Ångströms (Å). The two band nearly free electron model effectively represents the affect of the Ag band structure on the image electronic states. For electronic states in the substrate band gap, like image states at the benzene/Ag(111) interface (see Fig. 1), the solution in the Ag substrate corresponds to an exponentially

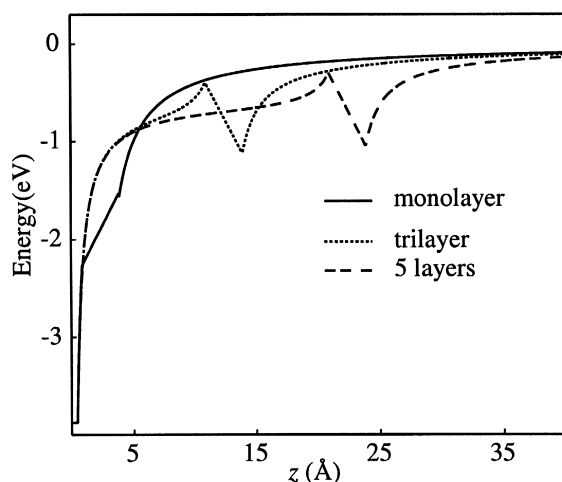


Fig. 7. The model potential for a monolayer, trilayer, and 5 layers of benzene adsorbed on Ag(111). The odd shape of the monolayer potential results from the narrow layer width, 2.4 Å, and the 3 Å interpolation width. Despite the sensitivity of the monolayer potential to the interpolation width, setting b to 1 Å did not significantly change the calculated binding energy and lifetime for the monolayer.

decaying evanescent wave (see Fig. 8). The slope and value of the evanescent wave solution are propagated numerically through the image potential in the layer and out into the vacuum. The numerical propagation uses a fourth and fifth order Runge-Kutta integrator with adaptive step sizes. The trial solutions are evaluated over a range of energies to identify solutions for which the wavefunction vanishes by 150 Å outside the layer. The lifetime of the image state is estimated from the product of the calculated electron density of the wavefunction in the metal (see Fig. 8) and an experimentally determined lifetime for an excited electron in bulk Ag at the energy of the image electronic state [25,26].

The benzene layer thickness, dielectric constant, and electron affinity represent the significant input parameters for the dielectric continuum model. The equilibrium distance of 2.4 Å between adsorbed benzene and the Ag(111) surface calculated by Anderson et al. is used to estimate the thickness of the benzene monolayer [17]. A 5 Å estimate for the thickness of each additional layer is derived from an averaged nearest neighbor distance in crystalline benzene [27]. The use of a bulk benzene dielectric constant and electron affinity is validated by the

weak benzene/Ag(111) electronic interaction discussed in Section 4. Ideally, the solid state dielectric constant and electron affinity of crystalline benzene would be used, but such values do not appear to exist in the literature. Condensed phase values, such as those of the liquid can be substituted. The dielectric constant and electron affinity of liquid n-heptane were successfully employed to model the binding

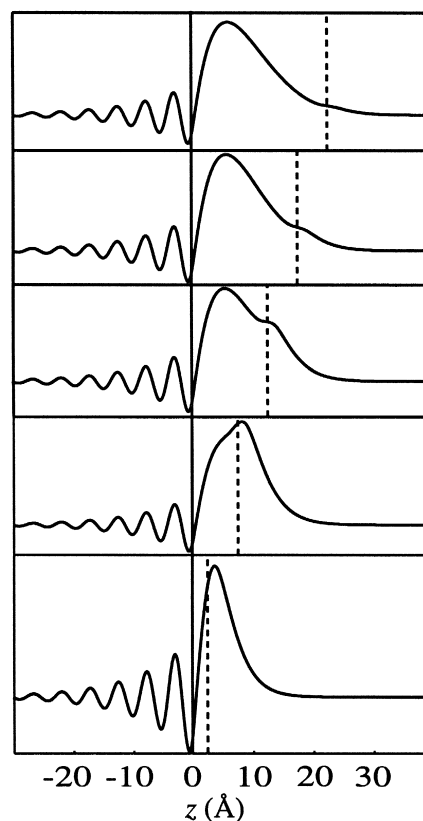


Fig. 8. The $n=1$ calculated wavefunction for 1, at the bottom, to 5 layers of benzene, at the top, adsorbed on Ag(111). The abscissa corresponds to the distance from the metal surface, with negative values of z residing in the substrate and positive values of z residing in the layer and vacuum. The straight vertical line represents the substrate/layer interface, while the dashed vertical line represents the layer/vacuum interface. The wavefunctions demonstrate that the electron resides primarily within the screened image potential in the benzene layer (see Fig. 7), which accounts for the layer independence of the binding energies and lifetimes for multilayer benzene. The sharp variations in the wavefunctions at the substrate/layer and layer/vacuum interfaces reflect the abrupt changes in the model potential and represent a major limitation of the dielectric continuum model.

energy and lifetime of image states at the n-heptane/Ag(111) interface [28]. The present calculation utilizes a liquid benzene dielectric constant of 2.3 [29]. An attractive electron affinity of 0.6 eV results in the closest agreement to experiment and differs little from the 0.5 eV electron affinity of liquid benzene [30]. The use of the -1.15 eV gas phase electron affinity of benzene for modeling the benzene/Cu(111) interface agrees with Velic et al.'s assignment of the benzene first electron affinity level above the vacuum energy, but gives image state lifetimes many orders of magnitude too long [8]. The use of a gas phase electron affinity in the dielectric continuum model should not correctly represent the layer electronic structure. The Xe/Ag(111) interface illustrates the importance of using condensed phase parameters when modeling interfacial unoccupied electronic structure. A model of the Xe/Ag(111) interface which uses the attractive electron affinity of solid state Xe reproduces experimentally observed Xe quantum wells [10,31], while the use of the repulsive gas phase electron affinity of Xe in the same model would not account for this result.

The calculated and experimentally measured binding energies and lifetimes of $n = 1$ for 1 to 5 layers of benzene are represented in Fig. 9. The calculated $n = 1$ binding energies and lifetimes change significantly from a monolayer to a bilayer of benzene, but vary little from 2 to 5 layers. Fig. 8 shows the calculated $n = 1$ wavefunctions for 1 to 5 layers. Inspection of the wavefunctions in Fig. 8 and the layer dependent model potential in Fig. 7 clearly shows the $n = 1$ image state electron to be trapped in the screened image potential within the benzene layer. The trapped image electron resides primarily within the first 2 benzene layers even when the coverage exceeds a bilayer, while the amplitude of the evanescent wave in the metal varies little with coverage for multilayer benzene. The lack of substantial change in the calculated $n = 1$ image state wavefunctions results in weakly changing binding energies and lifetimes for multilayer benzene. Trapping of the electron in the screened image potential in the layer results in a large image state electron density in the metal and $n = 1$ image state lifetimes comparable to those of the clean surface.

While treating the benzene layer as a structureless dielectric successfully models the $n = 1$ image state,

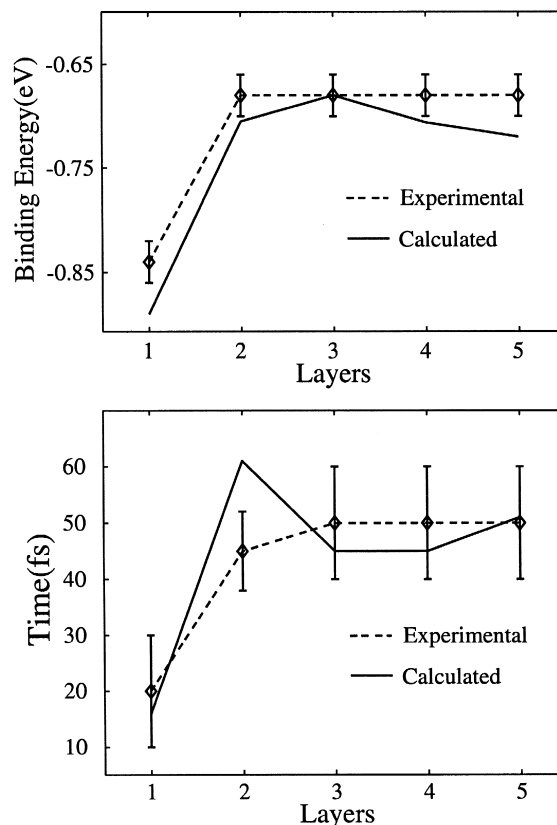


Fig. 9. Comparison between the calculated and measured $n = 1$ binding energies and lifetimes as a function of layer thickness. The weak oscillation in the calculated lifetime does not occur in the experimental data. The exaggerated layer dependent changes in the calculated lifetimes reflect the abrupt changes in the model potential at the layer/vacuum interface. Calculated image state lifetimes for the Xe/Ag(111) interface also exhibit exaggerated lifetime oscillations [31].

which has a binding energy larger than the layer electron affinity, the model does not appear capable of reproducing binding energies for image states above the electron affinity level. The dielectric continuum model predicts that the higher image state binding energies should increase as the coverage increases due to benzene quantum well formation. The $n = 2$ binding energies, -0.21 eV, -0.19 eV, and -0.19 eV for a monolayer, bilayer, and trilayer of benzene respectively, do not agree with the predicted binding energies. The dielectric continuum model exhibited a related inability to successfully predict the binding energies of image states above

the Xe band minimum for the Xe/Ag(111) interface [10]. The band properties of the overlayer influence quantum well formation, as reflected in the superior results for a layer potential that explicitly accounts for the Xe conduction band structure [10,31]. The inability of the dielectric continuum model to accurately account for the benzene band structure may cause the model to predict quantum well formation for $n = 2$ in the benzene layer when quantum well states do not appear experimentally, but the lack of sophisticated electronic band structure calculations which account for the electron localizing tendencies of aromatic molecular crystals [32] makes such a determination difficult. Despite the large electron density of the $n = 1$ image state in the benzene layer (see Fig. 9), the molecular anion forming tendencies of solid state benzene do not present themselves [9].

8. Conclusions

The layer dependent evolution of the benzene/Ag(111) unoccupied electronic structure and electron dynamics have been investigated with time and angle resolved TPPE. The binding energy and lifetime of the $n = 1$ image state has been measured for 1 to 5 layers of benzene. The free electron-like dispersions of the peaks in the angle resolved TPPE kinetic energy spectra make the assignment of the excitations as image electronic states clear. The unoccupied electronic states populated in our TPPE study resemble image states perturbed by the benzene layer electron affinity, rather than benzene anions perturbed by the image potential. The peak assigned to be the multilayer benzene first electron affinity level in the IPS study may be the peak assigned to be the multilayer benzene $n = 1$ image state [5]. The lack of angle resolved data in the IPS study makes distinguishing between localized molecular affinity levels and delocalized image states difficult. The IPS study involved many larger linear aromatic molecules adsorbed on Ag(111). The extension of time and angle resolved TPPE to include these larger molecules should further our understanding of the interaction between molecular affinity levels and the image potential. Adsorption of a monolayer of benzene moves the $n = 1$ image state

electron closer to the metal, as reflected in the increase in the $n = 1$ binding energy and the decrease in the $n = 1$ lifetime. Adsorption of a bilayer decreases the binding energy and increases the lifetime of the $n = 1$ image state. The lifetime and binding energy remain constant from a bilayer to 5 layers of benzene. A dielectric continuum model successfully reproduces these trends in $n = 1$ binding energy and lifetime.

Analysis of the model potential and the calculated wavefunctions shows the layer independence of the multilayer $n = 1$ lifetimes and binding energies to result from the trapping of the electron in the screened image potential within the benzene layer. The dielectric continuum model accounts for the influence of the benzene layer on the $n = 1$ image electronic states with a dielectric constant and a first electron affinity level. An attractive electron affinity of 0.6 eV gave the best agreement between experiment and calculation. Despite the similar binding energies and lifetimes for monolayer and bilayer $n = 1$ image states at the benzene/Cu(111) and the benzene/Ag(111) interfaces, Velic et al. used the benzene gas phase electron affinity of -1.15 eV in a dielectric continuum model calculation for benzene adsorbed on Cu(111) [8]. The repulsive gas phase electron affinity resulted in calculated lifetimes orders of magnitude too long. Benzene molecular anions did not appear in our TPPE study of the benzene/Ag(111) interface, despite the strong electron localizing tendencies of aromatic molecular crystals [9]. Identifying the circumstances under which molecular anions will and will not form represents an important issue in surface physics and chemistry. The extension of time and angle resolved TPPE to a wider variety of attractive electron affinity materials should advance our understanding of this issue and test the validity of dissociative electron transfer models of metal surface photochemistry.

Acknowledgements

This work was supported by the Director, Office of Energy Research, Office of Basic Energy Sciences, Chemical Sciences Division of the U.S. Department of Energy, under Contract No. DE-AC03-

76SF00098. The authors acknowledge NSF support for specialized equipment used in the experiments described herein.

References

- [1] W. Ho, *J. Phys. Chem.* 100 (1996) 13050.
- [2] J.W. Gadzuk, *Phys. Rev. Lett.* 76 (1996) 4234.
- [3] Y. Yang, *MRS Bulletin* 22 (1997) 31.
- [4] W.R. Salaneck, J.L. Brédas, *MRS Bulletin* 22 (1997) 46.
- [5] K.H. Frank, P. Yannoulis, R. Dudde, E.E. Koch, *J. Chem. Phys.* 89 (1988) 7569.
- [6] T. Munakata, T. Sakashita, M. Tsukakoshi, J. Nakamura, *Chem. Phys. Lett.* 271 (1997) 377.
- [7] T. Munakata, T. Sakashita, K.-I. Shudo, *J. Elec. Spect. Relat. Phenom.* 88-91 (1998) 591.
- [8] D. Velic, A. Hotzel, M. Wolf, G. Ertl, *J. Chem. Phys.* 109 (1998) 9155.
- [9] E.A. Silinsh, V. Capek, *Organic molecular crystals: interactions, localization, and transport phenomena*, American Institute of Physics, New York, 1994.
- [10] J.D. McNeill, R.L. Lingle Jr., R.E. Jordan, D.F. Padowitz, C.B. Harris, *J. Chem. Phys.* 105 (1996) 3883.
- [11] C.B. Harris, N.-H. Ge, R.L. Lingle Jr., J.D. McNeill, C.M. Wong, *Annu. Rev. Phys. Chem.* 48 (1997) 711.
- [12] Ph. Avouris, J.E. Demuth, *J. Chem. Phys.* 75 (1981) 4783.
- [13] R. Dudde, K.-H. Frank, E.-E. Koch, *Surf. Sci.* 225 (1990) 267.
- [14] L.E. Firment, G.A. Somorjai, *Surf. Sci.* 84 (1979) 275.
- [15] M. Xi, M.X. Yang, S.K. Jo, B.E. Bent, P. Stevens, *J. Chem. Phys.* 101 (1994) 9122.
- [16] X.-L. Zhou, M.E. Castro, J.M. White, *Surf. Sci.* 238 (1990) 215.
- [17] A.B. Anderson, M.R. McDevitt, F.L. Urbach, *Surf. Sci.* 146 (1984) 80.
- [18] Th. Fauster, W. Steinmann, *Electromagnetic waves: recent developments in research*, vol. 2. *Photonic Probes of Surfaces*, P. Halevi (Ed.), Elsevier, Amsterdam, 1995.
- [19] K. Giesen, F. Hage, F.J. Himpsel, H.J. Riess, W. Steinmann, N.V. Smith, *Phys. Rev. B* 35 (1987) 975.
- [20] R. Fischer, Th. Fauster, W. Steinmann, *Phys. Rev. B* 48 (1993) 15496.
- [21] N.-H. Ge, C.M. Wong, R.L. Lingle Jr., J.D. McNeill, K.J. Gaffney, C.B. Harris, *Science* 279 (1998) 202.
- [22] E.V. Chulkov, I. Sarriá, V.M. Silkin, J.M. Pitarke, P.M. Echenique, *Phys. Rev. Lett.* 80 (1998) 4947.
- [23] J. Osma, I. Sarriá, E.V. Chulkov, J.M. Pitarke, P.M. Echenique, *Phys. Rev. B* 59 (1999) 10591.
- [24] A. Hotzel, G. Moos, K. Ishioka, M. Wolf, G. Ertl, *Appl. Phys. B* 68 (1999) 615.
- [25] P.L. de Andres, P.M. Echenique, F. Flores, *Phys. Rev. B* 39 (1989) 10356.
- [26] A. Goldmann, W. Altmann, V. Dose, *Solid State Commun.* 79 (1991) 511.
- [27] D.E. Williams, Y. Xiao, *Acta Cryst. A* 49 (1993) 1.
- [28] R.L. Lingle Jr., N.-H. Ge, R.E. Jordan, J.D. McNeill, C.B. Harris, *Chem. Phys.* 205 (1996) 191.
- [29] D.R. Lide, (Ed.), *CRC Handbook of Chemistry and Physics*, 71st ed., CRC Press, Boca Raton, FL, 1990-1991.
- [30] Y. Nakato, M. Ozaki, H. Tsubomura, *J. Phys. Chem.* 76 (1972) 2015.
- [31] J.D. McNeill, R.L. Lingle Jr., N.-H. Ge, C.M. Wong, R.E. Jordan, C.B. Harris, *Phys. Rev. Lett.* 79 (1997) 4645.
- [32] R.M. Glaeser, R.S. Berry, *J. Chem. Phys.* 44 (1966) 3797.